Ultrasonic Waveguides for Quench Detection in HTS Magnets

M. Marchevsky, S. Prestemon, O. Lobkis, R. Roth, D. C. van der Laan, and J. D. Weiss

***Abstract*—High-temperature superconductors (HTS) are expected to have a major impact on the development of future particle accelerators and fusion energy systems. One of key challenges associated with HTS is a slow propagation of the normal zone that complicates early detection of thermal runaway (quench) in an HTS magnet using voltage-based techniques. Furthermore, fusion systems require field ramping rates up to several T/s under strong time-varying ac magnetic fields imposed on the conductor which makes voltage-based quench detection difficult or impractical. We propose an alternative non-voltage quench detection solution based upon monitoring ultrasonic wave propagation in a solid fiber-like flexible waveguide. The latter can be co-wound with the superconducting cable and carry acoustic waves over long distances. Acoustic waveguides allow for measuring local variation of strain or temperature in a way similar to optical fibers. However, unlike fiber-optic sensors, mechanical waveguides are constructed of robust materials and eliminate the need for expensive and complex signal receivers and data processing equipment. We will present our early developments in cryogenic ultrasonic waveguide technology, and discuss preliminary experiments conducted towards validating it for future use in practical HTS magnets.**

***Index Terms*—High-temperature superconductor magnets, quench, quench detection, ultrasonic waveguide, acoustic thermometry.**

I. Introduction

Recent progress in development and large-scale production of high-temperature superconductor (HTS) conductors enabled their increasing application in high-field magnets for high energy physics [1]–[4] and future fusion energy applications [5]. Among various challenges associated with the use of HTS conductors is the velocity of quench propagation that is one to two orders of magnitude lower in HTS than in their low-temperature superconductor counterparts [6], [7]. In applications like fusion where a significant ac background noise can be present due to plasma currents or where magnetic field needs to be ramped at high rate, the low velocity of quench propagation makes it difficult to detect a quench development timely using regular voltage-based quench detection techniques. This increases a probability of incurring thermal damage within HTS coils, and calls for a development of alternative quench detection techniques. Even in a situation where sensitive enough voltage-based quench detection is in place, achieving redundancy of quench detection can be important for critical applications.

Among various non-voltage quench detection and localization methods for HTS conductors and magnets, optical methods based on either discreet Fiber Bragg Gratings (FBG) sensors [8] or continuous ones based on Rayleigh back-scattering [9], [10] are well known. A clear advantage of using a continuous fiber sensor is that it allows for a distributed measurement of temperature along the entire length of superconducting coil winding and precise localization of the developing hot spots. However, known disadvantages are a fragility of the optical fibers, high costs of optical interrogators and need for a substantial computational power for monitoring long conductor lengths.

Another existing non-voltage quench detection technology is based on acoustic thermometry. The approach has been first pioneered in the 80's when various acoustic characteristics of superconducting magnets, such as mechanical resonances [11] or transfer function [12] were studied as function of hot spot development and quench. More recently, a diffuse wave ultrasonic approach to quench detection was demonstrated [13], [14] that relies on the temperature dependence of the diffuse ultrasonic wave (coda) [15] caused by the temperature dependence of the speed of sound. While this method works well for small coils and short ($\sim$1 m) length of HTS conductors, it becomes more challenging to apply to large magnets with a significant volume of the supporting mechanical structural element, as ultrasonic waves may then get a "shortcut" propagating through such structure, thus reducing sensitivity to hot spot development in the HTS conductor. An alternative approach would combine advantages of a distributed sensor like the optical fiber with simplicity and low implementation cost of the ultrasonic approach. Hence, in this work we propose the use of guided acoustic waves for detection of localized heating in HTS conductors. We demonstrate a practical implementation of the acoustic waveguide technology for temperature monitoring at cryogenic temperatures, and show preliminary results on using it for detection of quenches in a sample of HTS Conductor on Round Core (CORC) wire [16].

II. Technology

A. Acoustic Wave in a Solid-State Waveguide

When an acoustic / ultrasonic wave is excited in a solid mechanical structure of extended dimensions, certain wave

Manuscript received November 30, 2021; revised February 16, 2022 and March 7, 2022; accepted March 29, 2022. Date of publication March 31, 2022; date of current version April 25, 2022. This work was supported by US Magnet Development Program and the U.S. Department of Energy, Offices of Fusion Energy Sciences and High Energy Physics under Contract numbers DE-AC02-05CH11231, DE-SC0014009 and DE-SC0019934. *(Corresponding author: M. Marchevsky.)*

M. Marchevsky and S. Prestemon are with Lawrence Berkeley National Laboratory, Berkeley, CA 94720-8203 USA (e-mail: mmartchevskii@lbl.gov; soprestemon@lbl.gov).

O. Lobkis and R. Roth are with Etegent Technologies Ltd., Cincinnati, OH 45212 USA (e-mail: oleg.lobkis@etegent.com; richard.roth@etegent.com).

D. C. van der Laan and J. D. Weiss are with Advanced Conductor Technologies LLC, Boulder, CO 80301 USA and also with the University of Colorado, Boulder, CO 80301 USA (e-mail: danko@advancedconductor.com; jeremy@advancedconductor.com).

Color versions of one or more figures in this article are available at https://doi.org/10.1109/TASC.2022.3164035.

Digital Object Identifier 10.1109/TASC.2022.3164035

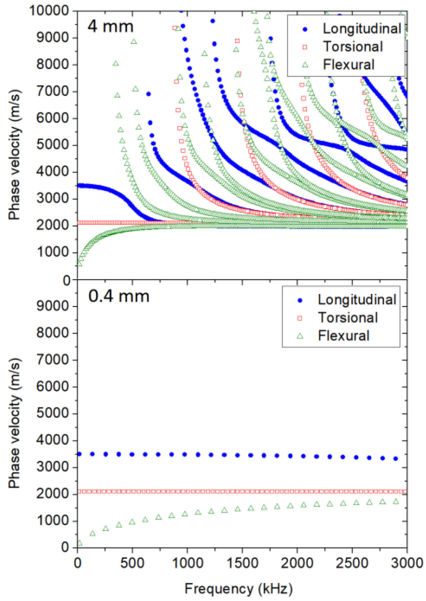

Fig. 1. Dispersion plots for brass acoustic waveguides of 4 mm diameter (top plot) and 0.4 mm diameter (bottom plot) calculated assuming material parameters: density r = 8600 kg/m^3, longitudinal sound velocity of v_l = 4700 m/s and shear sound velocity v_s = 2100 m/s. For the smaller diameter waveguide, the number of guided wave modes in the frequency range of 0–3 MHz is drastically reduced. Also, there exists a much wider range of nearly non-dispersive propagation for the longitudinal and flexural modes.

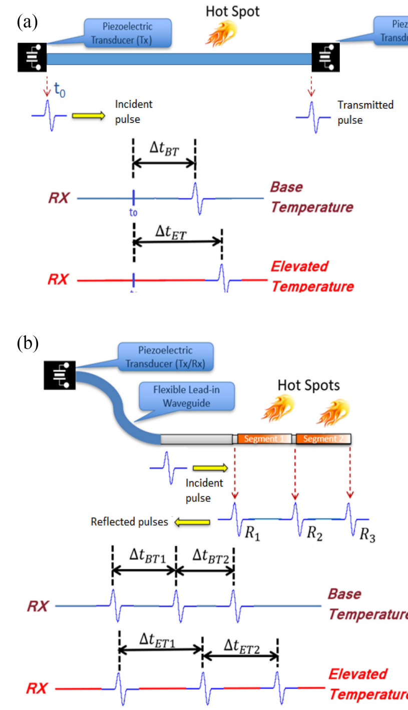

Fig. 2. (a) Detection of a hot spot along along the acoustic waveguide in transmission mode, by monitoring the delay in the pulse arrival due to the temperature dependence of the sound velocity. (b) Detection of hot spots in reflection mode. A time interval between the reflected pulses varies with the temperature of the corresponding waveguide segment, and is independent on the variations outside of that segment.

modes are able to propagate long distances along that structure. These modes are usually called guided waves, and they are often employed to detect mechanical flaws in pipes, cables and other similar extended structures supporting the guided wave propagation [17]. The simplest example of an acoustic waveguide is a solid metal rod (or wire), where guided wave propagation can be analytically described with the Pochhammer equation [18], [19]. Three kinds of guided waves: longitudinal, flexural and torsional can co-exist in a metal rod. If the phase velocity of the guided acoustic wave is plotted as a function of the excitation frequency, an extended frequency range can be identified for the longitudinal and torsional modes where dispersion is negligibly small. Therefore, acoustic excitations within that frequency range can propagate along the waveguide with a very little distortion, preserving high fidelity of the transmitted signal. In Fig. 1 dispersion plots calculated using GUIGUW software [20], [21] are shown for cylindrical brass waveguides of two different diameters, illustrating emergence of non-dispersive transmission in the thinner waveguides in a broad frequency range. While the torsional mode is fully non-dispersive independently of the waveguide diameter, it is somewhat difficult to excite efficiently in a thin wire using simple piezoelectric transducers. Therefore, in this work we employ the longitudinal mode for thermal sensing; this mode is nearly non-dispersive for a broad range of ultrasonic frequencies in waveguides of practical ~0.1–1 mm diameters, and has a higher propagating velocity compared to other modes.

B. Thermal Sensing Using Acoustic Waveguides

Thermal sensing using acoustic waveguides is generally a well-established method [22], [23]. It relies on the dependence of the sound velocity on temperature that is typically of the order of 10^{-4} K^{-1} for many common metals. To measure temperature variation along the waveguide, various schemes may be used. The simplest one is to repeatedly monitor propagation time of an acoustic pulse in transmission mode, thus measuring variation of the sound velocity averaged over the entire waveguide length (Fig. 2(a)). A more sophisticated approach involves placing a number of acoustic reflectors along the waveguide, and measuring arrival time variation of the reflected acoustic pulses (Fig. 2(b)). In this way, local temperature changes within a segment between a given pair of reflectors can be measured independently of the variations occurring elsewhere in the waveguide. This approach was adopted in the past to measure temperature distribution in extreme environments [24].

Several practical aspects should be considered when applying this technology at cryogenic temperatures and within a superconducting magnet structure. First of all, a cryogenic liquid (liquid nitrogen or liquid helium) may be surrounding the entire waveguide or a portion of it, which may lead to a leakage of the ultrasonic wave into the surrounding liquid resulting in attenuation of the signal. For example, in a 1 mm diameter titanium waveguide for the axially-symmetric lowest-order longitudinal mode L(01) at 2 MHz the attenuation coefficient K_i is ~20 m^{-1} and the ultrasonic wave can propagate only several centimeters before complete leakage into the liquid nitrogen. However, at 200 kHz the attenuation coefficient $K_i \sim 0.077$ m^{-1} and the propagation length increases to several meters. In liquid helium the leakage is about an order of magnitude less due to lower density and sound velocity values (assuming density $\rho_{LN2} =$ 0.804 g/cm^3, $\rho_{LHe} = 0.125$ g/cm^3, and velocity $v_{LN2} = 0.857$ mm/μs, $v_{LHe} = 0.18$ mm/μs).

A waveguide integrated with the magnet winding will be curved, and its wavenumber k_R can be then presented as $K_R =$

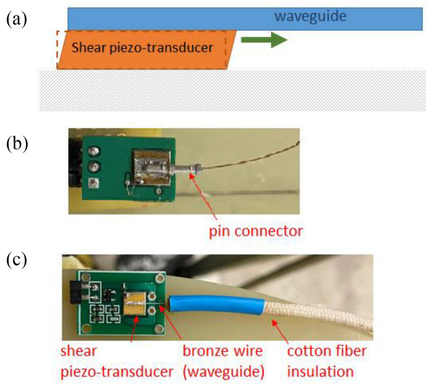

Fig. 3. (a) A sketch showing use of a shear wave piezo-transducer for exciting longitudinal acoustic waves in a wire waveguide. (b) A waveguide transmitter using a demountable pin connector. (c) A waveguide receiver built with a shear piezo-transducer integrated with a MOSFET-based cryogenic preamplifier in a single printed circuit board.

$\sqrt{K^2 - R^2}$ where K is the wavenumber of straight waveguide and R is a bending radius. The critical frequency at which guided waves become evanescent can then be estimated as $f = \nu/2\pi R$ [25]. For a copper waveguide with the phase velocity $\nu = 3.71$ mm/μs the critical frequency for $R = 20$ mm is $f =$ 30 kHz which is much lower than the expected operating frequency of several hundred kHz and guided waves should propagate through such bending radius without experiencing additional attenuation.

Performance of a practical quench detection depends on a good thermal link between the superconducting cable and waveguide. At the same time mechanical contact between these two objects should be minimal, in order to avoid ultrasonic wave leakage. This challenge may be potentially addressed by anchoring the waveguide to the conductor only at pre-defined reflection points of the waveguide, while making the reflectors from a high thermal conductivity material. Alternatively, a light powder or very soft yet thermally conductive material may be used to create a distributed random contact between the waveguide and conductor that would not support shear stresses associated with the longitudinal wave propagation.

C. Practical Implementation

We implemented our waveguide systems using bronze wires of various lengths and diameters driven by shear-mode piezoelectric transducers (Thorlabs, type PL5FB) (Fig. 3(a)). When a waveguide is soldered to a shear-mode piezoelectric plate, the longitudinal mode is preferentially excited. An alternative method to direct soldering of the waveguide is use of a demountable pin connector, as shown in Fig. 3(b). We found that such connectors do not introduce substantial attenuation or notable unwanted distortions into the acoustic signal. To ensure a better signal-to-noise ratio, we use cryogenic amplifiers integrated with the receiver transducers; the amplifier is based on a single MOSFET transistor and is similar in design to the one described in [26]. We apply rectangular pulses of 50–200 V in amplitude with a duration of 2-4 ms to the TX transducer using OSUN200 ultrasonic pulser, and record received signals in transmission mode using Picoscope 4824 USB oscilloscope. The data is then processed to determine the initial propagation time of the ultrasonic pulse through the waveguide, and a cross-correlation-based technique [13] is used to monitor its time shift continuously as ultrasonic pulses are being applied at a rate of 50 Hz. Temperature rise along the waveguide leads to a positive time shift (= delay) in the received waveform.

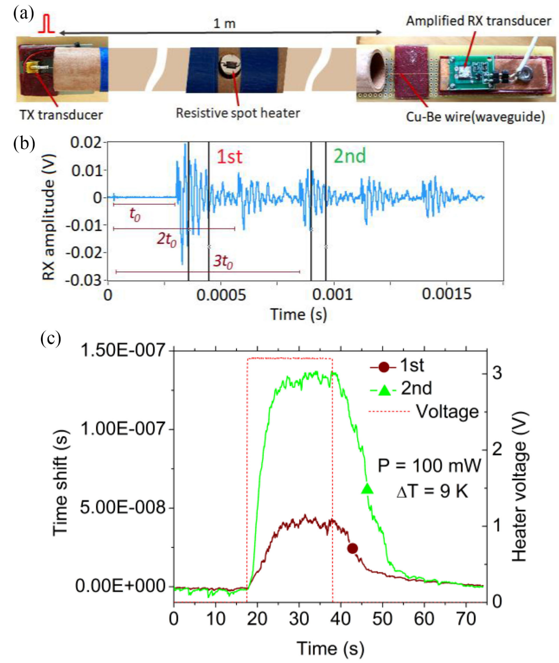

Fig. 4. (a) A sketch showing a test setup used to investigate thermal sensitivity of the waveguide at the ambient temperature conditions. (b) The RX waveform showing arrival of the signal and its multiple reflections from waveguide ends. Wave packets outlined in the plots with vertical markers correspond to an initial arrival of the longitudinal wave (1st) at time t_0 and the secondary arrival after the wave is reflected back from the TX transmitter side (2nd) at $3t_0$. (c) Time shift measured as a response to powering up the spot heater at 100 mW for ~20 s. Time shift accumulates with every pass of the wave along the waveguide thus yielding larger amplitude when secondary arrival wave packet was monitored.

III. Ambient Temperature Tests

We have constructed a simple setup to test thermal sensitivity of the acoustic waveguide at ambient temperature. A Cu-Be alloy wire of 0.076 mm diameter and 1.05 m length was used as a waveguide, and it was suspended inside a 1/2 inch ID fiberglass tube. The TX transducer was installed at one end and the amplified EX transducer at the other. At the middle of the waveguide a spot heater made of a 0.125 W 50 W resistor wrapped with copper foil was mounted; the waveguide was thermally anchored to this spot heater using thermal grease compound (Dow Corning 340). The setup is shown in Fig. 4(a).

In the first test, rectangular voltage pulses of 75 V in amplitude and 3.5 ms in duration were applied at a 50 Hz repetition rate to the RX transducer. The resulting RX waveform shows wave packets distinctly separated in time, corresponding to the arrival of the main longitudinal wave at time t_0, as well as its reflections from the spot heater (arriving at $2t_0$, $4t_0$, etc.) and from the TX end of the waveguide (arriving at $3t_0$, $6t_0$, etc.). The frequency content of the packets is dominated by post-pulsing ringing of the TX transducer. To perform temperature measurements, we monitored a portion of the 1st arriving wave packet (direct arrival) and the first reflection from the TX end of the waveguide. The latter packet travels the waveguide length three times, and therefore arrives to the RX transducer three times later than the directly incident wave. When the spot heater is powered at ~3 V, it dissipates 100 mW of power, and over a duration of about

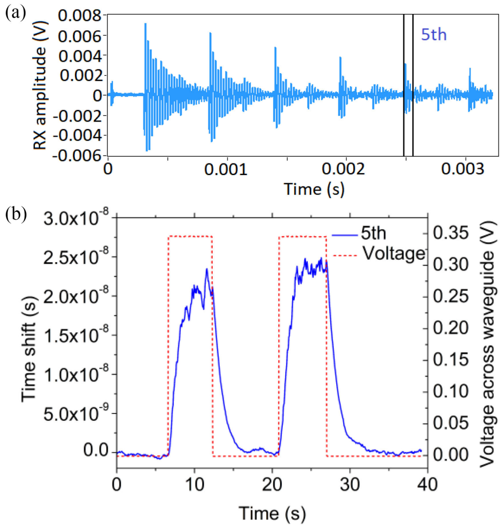

Fig. 5. (a) The RX waveform showing multiple end reflections of the longitudinal wave in the waveguide. Small amplitude reflections appearing in-between main reflection peaks are likely caused by a remaining minor deformation of the waveguide wire at the former spot heater location. The monitored wave marked with the vertical lines corresponds to the 5th arrival (after making full four back and forth reflections). (b) The time shift measured in response to applying 20 mA dc current, yielding ~6 mW of heating power in the waveguide.

20 s its temperature stabilizes at ~9 k above the ambient, as was measured using an infrared point thermometer. A distinct time shift associated with the local heating was measured in this experiment, yielding a magnitude of $\sim 4.2\times10^{-8}$ s for the direct wave and $\sim1.35\times10^{-7}$ s for the end-reflected one. The latter time shift is approximately three times larger than the first one, as expected given the fact that the reflected wave accumulates its thermally-induced delay three times when travelling along the waveguide three times; forward, back and forward again.

In the second test, we separated the waveguide wire from the spot heater, and applied constant current to it in order to induce uniform heating. This was done by connecting a current source (Stanford Research Instruments CS580) between the TX and RX termination points of the waveguide. Data from this experiment is shown in Fig. 5. For the applied current of 20 mA the end-to-end voltage measured across the waveguide was 295 mV, yielding 6 mW of heat dissipation. The measured time shift is ~2.2- 2.5×10^{-8} s.

A simple comparison between the two tests can be made. The 5th wave arrival corresponds to nine end-to-end wave travels along the waveguide, while the 2nd arrival corresponds to three end-to-end travels. This yields an expected factor of 3 in sensitivity improvements for the second test. Then, assuming time shift is directly proportional to the applied heating power, its expected value in the second test should be $(1.35\times10^{-7}\text{ s}) \times (6\text{ mW}/100\text{ mW}) \times 3 = 2.43\times10^{-8}$ s. This value is indeed very close to the one measured in experiment. Room temperature tests are thus mutually consistent, and provide a good estimate for the expected sensitivity of the technique towards quench detection applications.

IV. Quench Detection Test

A. Experimental Setup

To test the technique at realistic cryogenic conditions, a setup shown in Fig. 6(a) was built, aiming at detecting heating and ultimately quenching in a 50 cm-long sample of CORC HTS

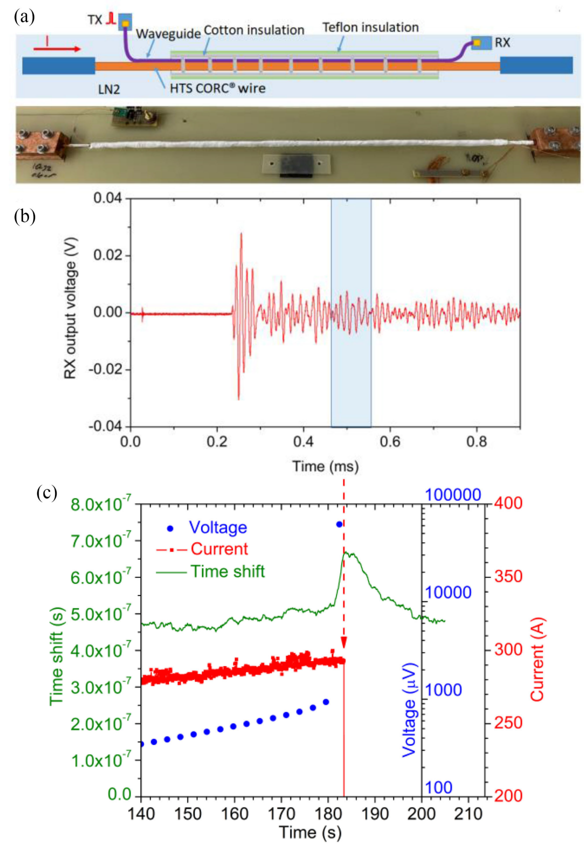

Fig. 6. (a) A sketch of the CORC wire testing setup (top) and the photo of the actual setup (bottom). (b) The RX waveform of the transmitted wave measured at 77k. The marked portion of the waveform was monitored for time during current ramping the cable sample. (c) The result of the quench experiment, showing the sample current, voltage and accumulated time shift as function of time. A clear rise in time shift is seen at quench (marked with an arrow), followed by a relaxation towards the base value upon sample cooling down to the temperature of the nitrogen bath.

conductor in liquid nitrogen. Our choice of CORC wire for this test was guided by use of such conductor for the HTS accelerator magnets presently developed at LBNL under the US Magnet Development Program. The CORC sample, manufactured by Advanced Conductor Technologies, comprises four 2-mm wide ReBCO tapes wound around a central copper core. The critical current of the sample at 77 k determined with 1 mV/cm voltage criterion is 235 A. We have instrumented this conductor with a waveguide sensor made out of a phosphor bronze wire 0.22 mm in diameter. The waveguide wire was placed straight along the entire conductor length, and then secured to it using cotton threads at ~5 cm intervals. Then a cotton sheath insulation was wrapped around the instrumented conductor, and an additional layer of PTFE tape insulation was wound over it. This arrangement allowed for a good transmission of the acoustic wave along the mounted waveguide, yet provided some basic heat insulation to it by reducing heat exchange between the conductor and nitrogen bath, allowing the waveguide to reach higher temperatures in the event of a quench. The same RX transducer as in the room temperature test was used, while another RX transducer was built around a different type of a MOSFET that has a wider operational frequency bandwidth and lower background noise. Rectangular pulses of 150 V amplitude and 4 ms duration at a 50 Hz repetition rate was applied at liquid nitrogen temperature to the TX transducer, resulting in a clean and stable RX waveform as shown in Fig. 6(b). However, due to an extended contact area between the waveguide and the cable, this waveform has a more complex shape than those obtained in the room temperature tests. We ramped up the CORC sample current at a constant rate until quench was detected and the power supply was subsequently turned off. Conductor current, conductor voltage (plotted in the logarithmic scale) and time shift are shown in Fig. 6(c) together as function of the elapsed time. While voltage across the CORC wire was increasing, a slight increase in time shift was observed as well, but only for currents that are 10–15 A below the quench. When quench occurred at 293 A, the sample voltage jumped to 60 mV yielding power dissipation of $\sim$17.5 W for approx. 0.5 s. This heat release resulted in a clearly detectable time shift variation of $\sim 1.5\times10^{-7}$ s, followed by an approximately 20 s long relaxation towards the base temperature level after turning off the current. These results clearly demonstrate an ability of the waveguide sensor to detect a quench. However, for practical use its thermal sensitivity needs to be increased to be able to sense pre-quench heating in the conductor more clearly. A better thermal link between the waveguide and CORC wire is necessary to achieve this, and further investigation will be carried out in search for a more suitable waveguide insulation material.

V. Conclusion

We investigated use of acoustic guided waves for thermal sensing in both ambient and cryogenic environments, and developed a cryogenically-robust waveguide thermometry system around shear-wave piezoelectric transducers and integrated MOSFET-based amplifiers. Sensitivity of this system to localized and large-scale thermal variations have been quantified, and preliminary experiments were conducted demonstrating successful use of this technology for detection of quenches in practical HTS conductor at liquid nitrogen temperature. The technique has a potential of becoming a robust and less expensive alternative to the fiber-optics-based quench detection. To enable its integration with practical HTS magnets, more research is required on developing a waveguide acoustic insulation that would efficiently conduct heat but prevent leakage of ultrasonic waves into the HTS conductor and surrounding structural elements. In the future, we also plan to investigate a pulse-echo mode of time shift detection, aiming at improving detection sensitivity while also enabling localization of the developing hot spots. It appears plausible to place multiple (10+) reflectors along the waveguide without having a significant degradation of the reflected signal amplitude. We will further explore this approach by optimizing reflector density and distribution to improve localization capabilities of the technique.

Acknowledgment

The authors would like to thank Tim Bogdanoff for fabrication of the support structure used in the CORC wire experiment. M. Marchevsky is thankful to Reed Teyber and Geon Seok Lee for stimulating discussions.

References

[1] L. Rossi and C. Senatore, "HTS accelerator magnet and conductor development in Europe," *Instruments*, vol. 5, no. 1, Feb. 2021, Art. no. 8.

[2] G. A. Kirby *et al.*, "Accelerator-quality HTS dipole magnet demonstrator designs for the eucard-2 5-T 40-mm clear aperture magnet," *IEEE Trans. Appl. Supercond.*, vol. 25, no. 3, Jun. 2015, Art. no. 4000805.

[3] R. Gupta *et al.*, "Hybrid high-field cosine-theta accelerator magnet R&D with second-generation HTS," *IEEE Trans. Appl. Supercond.*, vol. 25, no. 3, Jun. 2015, Art. no. 4003704.

[4] E. Todesco, L. Bottura, G. De Rijk, and L. Rossi, "Dipoles for high-energy LHC," *IEEE Trans. Appl. Supercond.*, vol. 24, no. 3, Jun. 2014, Art. no. 4004306.

[5] M. J. Wolf, C. Ebner, W. H. Fietz, R. Heller, D. Nickel, and K.-P. Weiss, "High temperature superconductors for fusion applications and new developments for the HTS CroCo conductor design," *Fusion Eng. Des.*, vol. 172, Nov. 2021, Art. no. 112739.

[6] X. Wang *et al.*, "Normal zone initiation and propagation in Y-Ba-Cu-O coated conductors with CU stabilizer," *IEEE Trans. Appl. Supercond.*, vol. 15, no. 2, pp. 2586–2589, Jun. 2005.

[7] J. van Nugteren, M. Dhallé, S. Wessel, E. Krooshoop, A. Nijhuis, and H. ten Kate, "Measurement and analysis of normal zone propagation in a ReBCO coated conductor at temperatures below 50 K," *Phys. Procedia*, vol. 67, pp. 945–951, 2015.

[8] A. Chiuchiolo *et al.*, "Cryogenic-temperature profiling of high-power superconducting lines using local and distributed optical-fiber sensors," *Opt. Lett.*, vol. 40, no. 19, pp. 4424–4427, Oct. 2015.

[9] F. Scurti, S. Ishmael, G. Flanagan, and J. Schwartz, "Quench detection for high temperature superconductor magnets: A novel technique based on Rayleigh-backscattering interrogated optical fibers," *Supercond. Sci. Technol.*, vol. 29, no. 3, Mar. 2016, Art. no. 03LT01.

[10] F. Scurti and J. Schwartz, "Optical fiber distributed sensing for high temperature superconductor magnets," in *Proc. 25th Opt. Fiber Sensors Conf.*, Apr. 2017, pp. 1–4.

[11] T. Ishigohka, O. Tsukamoto, and Y. Iwasa, "Method to detect a temperature rise in superconducting coils with piezoelectric sensors," *Appl. Phys. Lett.*, vol. 43, no. 3, pp. 317–318, 1983.

[12] A. Ninomiya, K. Sakaniwa, H. Kado, T. Ishigohka, and Y. Higo, "Method to detect a temperature rise in superconducting coils with piezoelectric sensors," *Appl. Phys. Lett.*, vol. 43, no. 2, pp. 317–318, Aug. 1983.

[13] M. Marchevsky and S. A. Gourlay, "Acoustic thermometry for detecting quenches in superconducting coils and conductor stacks," *Appl. Phys. Lett.*, vol. 110, no. 1, Jan. 2017, Art. no. 012601.

[14] M. Marchevsky, E. Hershkovitz, X. Wang, S. A. Gourlay, and S. Prestemon, "Quench detection for high-temperature superconductor conductors using acoustic thermometry," *IEEE Trans. Appl. Supercond.*, vol. 28, no. 4, Jun. 2018, Art. no. 4703105.

[15] R. L. Weaver and O. I. Lobkis, "Temperature dependence of diffuse field phase," *Ultrasonics*, vol. 38, no. 1–8, pp. 491–494, Mar. 2000.

[16] D. C. van der Laan, L. F. Goodrich, and T. J. Haugan, "High-current DC power transmission in flexible RE–$Ba_2Cu_3O_{7-\delta}$ coated conductor cables," *Supercond. Sci. Technol.*, vol. 25, no. 1, Jan. 2012, Art. no. 014003.

[17] J. L. Rose, "Ultrasonic waves in solid media," *J. Acoust. Soc. Amer.*, vol. 107, no. 4, pp. 1807–1808, Apr. 2000.

[18] L. Pochhammer, "Uber die fortpflanzungsgeschwindigkeiten kleiner schwingungen in einem unbegrenzten isotropen kreiszylinder," *J. Reine Angewandte Math*, vol. 81, pp. 324–336, 1876.

[19] J. Zemanek Jr, "An experimental and theoretical investigation of elastic wave propagation in a cylinder," *J. Acoust. Soc. Amer.*, vol. 51, no. 1B, pp. 265–283, Jan. 1972.

[20] A. Marzani, "A Software for the Computation of Acoustic Waves in Cylindrical, Plate and Arbitrary Cross-Section Waveguides," in *Proc. 13a Congresso Nazionale Sulle Prove Non Distruttive Monitoraggio E Diagnostica Aipnd*, Roma, Italia, 1996.

[21] P. Bocchini, A. Marzani, and E. Viola, "Graphical user interface for guided acoustic waves," *J. Comput. Civil Eng.*, vol. 25, no. 3, pp. 202–210, May 2011.

[22] T. Y. Wong, Y. Tang, F. Zou, and Z. Su, "An ultra-high accuracy temperature measurement method using acoustic waveguide," *IEEE Sens. J.*, vol. 21, no. 3, pp. 2618–2626, Feb. 2021.

[23] Y. Wang, F. Zou, and F. B. Cegla, "Acoustic waveguides: An attractive alternative for accurate and robust contact thermometry," *Sens. Actuators A Phys.*, vol. 270, pp. 84–88, Feb. 2018.

[24] Y. Jia and M. Skliar, "Ultrasonic measurements of temperature distribution and heat fluxes across containments of extreme environments," presented at the 2019 IEEE Int. Ultrason. Symp., Glasgow, U.K., pp. 940–943, Oct. 2019, doi: 10.1109/ultsym.2019.8925643.

[25] M. A. Isakovitch and L. N. Komarova, "Longitudinal-flexural waves in a thin rod," *Sov. Phys.—Acoust. (Akusticheskii Zhurnal)*, vol. 13, no. 4, pp. 580–583, 1967.

[26] M. Marchevsky, G. Sabbi, H. Bajas, and S. Gourlay, "Acoustic emission during quench training of superconducting accelerator magnets," *Cryogenics (Guildf.)*, vol. 69, pp. 50–57, Jul. 2015.